A new clustering algorithm for PolSAR images segmentation

Violeta Roizman
L2S / CentraleSupélec, France
Universidad de Buenos Aires, Argentina
violeta.roizman@centralesupelec.fr

Gordana Draskovic
L2S / CentraleSupélec
University Paris-Saclay, France
gordana.draskovic@l2s.centralesupelec.fr

Frédéric Pascal
L2S / CentraleSupélec
University Paris-Saclay, France
frederic.pascal@centralesupelec.fr

***Abstract*—This paper deals with polarimetric synthetic aperture radar (PolSAR) image segmentation. More precisely, we present a new robust clustering algorithm designed for non-Gaussian data. The algorithm is based on an expectation-maximization approach. Its novelty is that, in addition to the estimation of each cluster center and covariance matrix, it also provides for each observation an estimation of the scale parameter, allowing a better flexibility when assigning each observation in one cluster. The method performances are evaluated on both simulated and real multi-looked PolSAR data. It is demonstrated that the algorithm outperforms the classical clustering algorithms such as k-means and GMM (Gaussian-based EM algorithm) in various scenarios.**

I. Introduction

The main goal of data clustering is to divide the data in different groups, called clusters, basing on the similarities between them. In the context of so-called model-based clustering algorithms, all data points from the same cluster are considered as sampled from one distribution with fixed parameters. A widely used multivariate probabilistic model is the Gaussian Mixture Model (GMM), which represents the distribution of the data as a random variable given by a mixture of Gaussian distributions. Consequently, all points drawn from one of these normal distributions are considered to belong to the same cluster. The parameters of this model are usually estimated using the two-step iterative Expectation-Maximization (EM) algorithm [1], based on the maximization of the likelihood. For GMM model, the EM algorithm provides closed-form expressions for the estimators of the mean and covariance matrix of each cluster.

However, it has been shown that this EM version can have really poor performances in the presence of noise (additive to the GMM) or high heterogeneous data. This can be explained by the non-robustness of the estimators computed in the algorithm: the empirical means and the sample covariance matrices (SCM). In order to improve the performance, two main strategies were developed. One consists in modifying the model to take into account any additive noise and the other one is to change the GMM for a mixture of non-Gaussian distributions leading to robust estimators that are able to deal with outliers or heterogeneous data. We are particularly interested in robustness because of the noisy nature of the PolSAR images we want to analyze and, in this case, we consider the latter class of algorithms. This decision is mainly based on the fact that non-Gaussian distributions have been successfully used to model real data behaviors in various radar applications [2], [3].

In Machine Learning, image segmentation is a classical clustering application. The goal is to segment the image in parts that have common characteristics. For example, in the case of color compressing, the goal is to detect sets of pixels that have similar colors so that the image can be accurately represented with a smaller amount of colors (one per cluster). In the case of PolSAR images, our objective is to segment field images by land use [4], [5]. In order to achieve this goal, we adapt the flexible and robust algorithm presented in [6] and we applied it on images by considering patches of pixels.

The rest of the paper is organized as follows. In section 2, we present the theoretical background of PolSAR images and the robust theory on top of which our algorithm is constructed. Section 3 describes the design of our method. Section 4 is devoted to the experimental results, which allow us to show the improved performance of our method for different simulated PolSAR images in comparison with other commonly used methods such as k-means. Finally, our conclusions are stated in section 5.

Notation: Vectors (resp. matrices) are denoted by boldfaced lowercase letters (resp. uppercase letters). $\mathbf{A}^T$ represents the transpose of $\mathbf{A}$, $|\mathbf{A}|$ represents the determinant of $\mathbf{A}$ and $\text{tr}(\mathbf{A})$ represents the trace of $\mathbf{A}$. $\mathcal{N}(0, \mathbf{I}_m)$ denotes the m-variate Gaussian distribution with zero-mean and covariance matrix equal to the identity matrix of dimension m.

II. Theoretical background

A. PolSAR images

Polarimetric SAR sensors measure the amplitude and phase of backscattered signals in four combinations of the linear

Work of F. Pascal has been partially supported by DGA under grant ANR-17-ASTR-0015. Work of G. Draskovic has been supported by DIGITEO Grant 2016-1277D-SERTI

received and transmitted polarizations: horizontal-horizontal (HH), horizontal-vertical (HV), vertical-horizontal (VH) and vertical-vertical (VV). These signals form the complex scattering matrix $\mathbf{S}$

$$\mathbf{S} = \begin{bmatrix} S_{HH} & S_{HV} \\ S_{VH} & S_{VV} \end{bmatrix}$$

Thanks to the reciprocity theorem, in the monostatic case (when the same antenna is used as transmitter and receiver) we assume that the cross-pol channels of the scattering matrix are equal, that is $S_{HV} = S_{VH}$. Therefore, the scattering matrix $\mathbf{S}$ can be rewritten to form a scattering vector as follows

$$\mathbf{k}_L = \begin{bmatrix} S_{HH} & \sqrt{2}S_{HV} & S_{VV} \end{bmatrix}^T \quad (1)$$

or equivalently

$$\mathbf{k}_P = \frac{1}{\sqrt{2}} \begin{bmatrix} S_{HH} + S_{VV} & S_{HH} - S_{VV} & 2S_{HV} \end{bmatrix}^T . \quad (2)$$

Because of the random nature of PolSAR images, the vector $\mathbf{k}$ has been usually modeled as a zero-mean complex Gaussian circular process. Denosing or clustering PolSAR data then consist in estimating the covariance matrix of the vector $\mathbf{k}$ in each pixel of the image. To that end, the well-known sample covariance matrix has been widely employed. However, the modern PolSAR data provided by high resolution SAR systems exhibit highly heterogeneous nature that can not be described by the classical Gaussian model. Consequently, new, more complex, models appeared. One of them, the scalar-texture model, has been designed in order to provide the additional parameter able to describe different scenarios occurred in PolSAR images. In the following section, we introduce the scalar texture model, also known as compound-Gaussian model, and its generalization given by elliptical distributions class.

B. Data model

Given $\chi = \{\mathbf{x}_i\}_{i=1}^n$ a set of data points in $\mathbb{R}^m$ we consider points as samples from a mixture of distributions with the following probability density function (pdf):

$$f(\mathbf{x}) = \sum_{k=1}^{K} \pi_k f_{\theta_k}(\mathbf{x}) \quad \text{with} \quad \sum_{k=1}^{K} \pi_k = 1, \quad (3)$$

where π_k represents the proportion of the k^{th} distribution in the mixture and f_{θ_k} its pdf depending on the parameters grouped in θ_k. We assume that $f_{\theta_k}(\mathbf{x}_i)$ is the pdf of Elliptically Symmetric (ES) distributions. An m-dimensional random vector $\mathbf{x}_i$ from the k^{th} distribution is ES-distributed if its pdf can be written as

$$f_{\theta_k}(\mathbf{x}_i) = C|\mathbf{\Sigma}_k|^{-\frac{1}{2}} g_{\mathbf{x}_i}\left((\mathbf{x}_i - \boldsymbol{\mu}_k)^T \mathbf{\Sigma}_k^{-1} (\mathbf{x}_i - \boldsymbol{\mu}_k)\right) \quad (4)$$

where C is a constant, $g_{\mathbf{x}_i} : [0, \infty) \to [0, \infty)$ is any function (called the density generator) such that (4) defines a pdf, $\boldsymbol{\mu}_k$ is the location parameter (mean) and $\mathbf{\Sigma}_k$ is the scatter matrix. The matrix $\mathbf{\Sigma}_k$ reflects the structure of the covariance matrix of X_i (the covariance matrix is equal to $\mathbf{\Sigma}_k$ up to a scale factor if the distribution has a finite second-order moment, see [7] for details). This is denoted $ES(\boldsymbol{\mu}_k, \mathbf{\Sigma}_k, g_{\mathbf{x}_i}(.))$.

These models admits a Stochastic Representation given as follows: $\mathbf{x} \sim ES(\boldsymbol{\mu}_k, \mathbf{\Sigma}_k, g_{\mathbf{x}_i}(.))$ if and only if it admits the following stochastic representation [8]

$$\mathbf{x} \overset{d}{=} \boldsymbol{\mu}_k + \sqrt{Q}\mathbf{A}_k\mathbf{u}, \quad (5)$$

where the non-negative real random variable Q, called the modular variate, is independent of the random vector $\mathbf{u}$ that is uniformly distributed on the unit m-sphere and $\mathbf{\Sigma}_k = \mathbf{A}_k\mathbf{A}_k^T$ is a factorization of $\mathbf{\Sigma}_k$.

ES distributions include the class of compound-Gaussian distributions. This particular family displays a random vector as an affine transformation of Gaussian process represented as follows

$$\mathbf{x}_i = \boldsymbol{\mu}_k + \sqrt{\tilde{\tau}_{ik}}\mathbf{A}_k\mathbf{g}_i, \quad (6)$$

where $\boldsymbol{\mu}_k$ corresponds to the mean, $\tilde{\tau}_{ik}$ is a positive random variable independent from $\mathbf{g}_i$, $\mathbf{g}_i \sim \mathcal{N}(0, \mathbf{I}_m)$ and $\mathbf{A}_k\mathbf{A}_k^T = \mathbf{\Sigma}_k$. Generally, some one-dimensional constraints on $\mathbf{\Sigma}_k$ is assumed for identifiability (between $\tilde{\tau}_{ik}$ and $\mathbf{\Sigma}_k$) conditions. In this work, we assume $tr(\mathbf{\Sigma}_k) = m$ (See [**?**] for more details). It is important to notice that since we consider a mixture of distribution, the (unknown) pdf of $\tilde{\tau}_{ik}$ can be different from one cluster to an other, explaining the notation involving an extra index k.

In the following, we do not set a particular distribution for $\tilde{\tau}_{ik}$ in Eq. (6) to estimate the cluster distribution in a parametric way. Instead, we model each cluster in an approximated way. We assume that each data point $\mathbf{x}_i \in \mathbb{R}^m$, from the cluster j of the mixture, is the result of multiplying a sample from a multivariate zero-mean Gaussian by a deterministic constant [**?**] and a consequent translation, i.e. it can be written as

$$\mathbf{x}_i = \boldsymbol{\mu}_k + \sqrt{\tau_{ik}}\mathbf{A}_k\,\mathbf{g}_i, \quad (7)$$

with the mean $\boldsymbol{\mu}_k$ a real vector, τ_{ik} a **deterministic constant** or parameter, $\mathbf{g}_i \sim \mathcal{N}(0, \mathbf{I}_m)$ and $\mathbf{A}_k\mathbf{A}_k^T = \mathbf{\Sigma}_k$ with $\text{tr}(\mathbf{\Sigma}_k) = m$. The proposed model can be seen as a general compound-Gaussian distribution conditionally to the texture parameter $\tilde{\tau}_{ik} = \tau_{ik}$.

Consequently, the data model considered for developing the clustering algorithm is the mixture model defined in Eq. (3) where $\theta_k = (\boldsymbol{\mu}_k, \mathbf{\Sigma}_k, \{\tau_{ik}\}_{i=1,..,N})$ for $k = 1, ..., K$. When comparing to a classical EM algorithm, this data modelling requires (in the M step) the estimation of all the τ_{ik}'s parameters leading to different estimators for the mean and the covariance matrix. Details can be found in [6].

III. Algorithm

The proposed algorithm, called R-EM for robust EM algorithm, is designed to segment images with the presence of

noise. In particular, we focus our method on PolSAR images. As this type of signals are complex valued zero-mean images, we then consider the amplitude real values to segment these images with our method and other classic methods as k-means and EM for GMM. We first smooth the data with small patches because the resulting amplitude real value is a very noisy signal.

Our algorithm has the same general structure as the two-step classical EM algorithm. Some distinctive characteristics of this algorithm are the recursive equations for the parameter estimations and the adaptation for images of τ updates. More precisely, we iteratively solve a fixed-point equation system derived from the expected likelihood in the maximization step that results in a robust estimation of the various parameters (see [6] for technical details). The equations corresponding to this equation system are in line 12 and line 13 of Algorithm 1 and correspond to the Tyler's M-estimators of the mean and the covariance matrix [9], [10]. On the other hand, we consider a patch of pixels to take advantage of the local structure of the image. Each patch represents the squared neighborhood of the pixel where it is centered and is supposed to be somehow homogeneous. Based on the later idea, we compute the estimation of the τ_i parameter of each pixel as the trimmed mean of all the pixels that belong to the corresponding patch. Even though we smooth the image before applying the clustering method, the trimming technique helps to discard some extreme values that remain in the data even after the smoothing.

Regarding the additional parameters that have to be tuned, different sizes for the patches have been tested for the texture estimation: $3 \times 3, 5 \times 5$ and 7×7. Additionally, we have also explored different strategies for the τ estimation: mean, median and trimmed mean over the patch. The trimmed mean has been kept as shown in Algorithm 1.

Algorithm 1: Scheme of the proposed R-EM algorithm

Input : Data $\chi = \{\mathbf{x}_i\}_{i=1}^n$, K the number of clusters
Output: Clustering labels $\mathcal{Z} = \{z_i\}_{i=1}^n$

1 Set initial random values $\theta^{(0)}$;
2 $l \leftarrow 1$;
3 **while** *not convergence* **do**
4 **E:** For each $1 \leq k \leq K$ and $1 \leq i \leq n$ compute:
5
$$p_{ik}^{(l)} = \frac{\pi_k^{(l-1)} f_{\theta_{ik}^{(l-1)}}(\mathbf{x}_i)}{\sum_{j=1}^{K} \pi_j^{(l-1)} f_{\theta_{ij}^{(l-1)}}(\mathbf{x}_i)};$$
6 **M:**
7 For each $1 \leq k \leq K$:
8 Update $\pi_k^{(l)} = \frac{1}{n}\sum_{i=1}^n p_{ik}^{(l)}$;
9 Update $w_{ik}^{(l)} = \frac{p_{ik}^{(l)}}{\sum_{l=1}^n p_{lk}^{(l)}}$;
10 Set $\boldsymbol{\mu}_k^{(')} = \boldsymbol{\mu}_k^{(l-1)}$ and $\boldsymbol{\Sigma}_k^{(')} = \boldsymbol{\Sigma}_k^{(l-1)}$;
11 **while** *not convergence* **do**
12
$$\boldsymbol{\mu}_k^{('')} = \frac{\sum_{i=1}^{n} \frac{p_{ik}^{(l)} \mathbf{x}_i}{(\mathbf{x}_i - \boldsymbol{\mu}_k^{(')})^T (\boldsymbol{\Sigma}_k^{(')})^{-1} (\mathbf{x}_i - \boldsymbol{\mu}_k^{(')})}}{\sum_{i=1}^{n} \frac{p_{ik}^{(l)}}{(\mathbf{x}_i - \boldsymbol{\mu}_k^{(')})^T (\boldsymbol{\Sigma}_k^{(')})^{-1} (\mathbf{x}_i - \boldsymbol{\mu}_k^{(')})}};$$
13
$$\boldsymbol{\Sigma}_k^{('')} = m \sum_{i=1}^{n} \frac{w_{ik}^{(l)} (\mathbf{x}_i - \boldsymbol{\mu}_k^{('')})(\mathbf{x}_i - \boldsymbol{\mu}_k^{('')})^T}{(\mathbf{x}_i - \boldsymbol{\mu}_k^{('')})^T (\boldsymbol{\Sigma}_k^{(')})^{-1} (\mathbf{x}_i - \boldsymbol{\mu}_k^{('')})};$$
14 **end**
15 Update $\boldsymbol{\mu}_k^{(l)} = \boldsymbol{\mu}_k^{('')}$ and $\boldsymbol{\Sigma}_k^{(l)} = \boldsymbol{\Sigma}_k^{('')}$;
16 **For each** pixel x_i:
17 **For each** pixel $\mathbf{x}_t$ in the patch of $\mathbf{x}_i$:
18
$$\tau_{tk}^{(l)} = \frac{(\mathbf{x}_t - \boldsymbol{\mu}_k^{(l)})^T (\boldsymbol{\Sigma}_k^{(l)})^{-1} (\mathbf{x}_t - \boldsymbol{\mu}_k^{(l)})}{m};$$
19 Set $\tau_{ik}^{(l)} = trimmedmean(\{\tau_{tk}^{(l)}\}_t)$;
20 $l \leftarrow l + 1$;
21 **end**
22 Sample z_i from a multinomial distribution $\mathcal{M}(p_{i1}, ..., p_{iK})$ to assign $\mathbf{x}_i$ to a cluster;

IV. EXPERIMENTS

In this section, we present the results obtained for simulated and real PolSAR data.

A. Simulated data

The original clusters have been generated using a Markov Random Field (MRF) following a Gibbs distribution as in [11]. A polarimetric behavior has been assigned to the different clusters of the designed images. The matrices have been sampled from the PolSAR data as explained in [11]. The procedure is the following.

First, we choose the number of polarimetric clusters K. A ground truth (original clusters) is generated using a MRF. For each cluster, one of the seven possible polarimetric signatures is randomly assigned and the Gaussian speckle noise is generated according to them. The exact values of covariance matrices can be found in [11]. Then, we generate several noisy PolSAR images in order to obtain multi-looked images. The multi-looked images are obtained averaging several speckle images. An example of generated classes and simulated multi-looked PolSAR data is given in Figure 1. The number of classes is set to 3. The multi-looked data are obtained averaging 6 speckle images.

The segmentation is performed by k-means, GMM and the robust EM algorithm denoted as R-EM. Figure 2 displays the obtained results. First column displays the results obtained with k-means method, second column displays the results

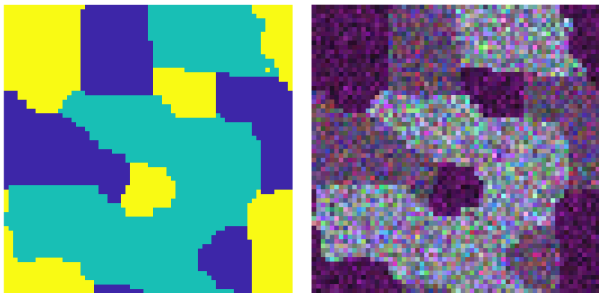

Figure 1: An example of original classes (left) and simulated 6-looked PolSAR data (right)

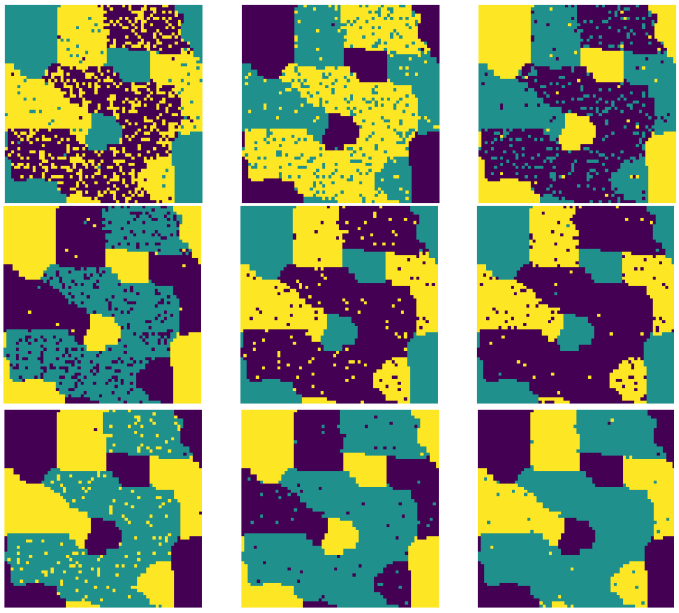

Figure 2: Clustering results for multi-looked data PolSAR data. From left to right: results for k-means, GMM and R-EM, from top to bottom: results for 6,9 and 12-looked PolSAR data

with GMM and third column displays the results obtained with R-EM. First row summarizes the results obtained for 6-looked data. One can note that the k-means method provides "noisy" results while R-EM gives the best clustering results. This is even more obvious for 9-looked (second row) and 12-looked data (third row). From third row, one can see that the results obtained with R-EM contain an insignificant number of misclassified pixels. To confirm these results, Table I provides the percentage of correct classification for the three methods. These results are in favor of the proposed algorithm whose improved performance is due to its flexibility (thanks to the τ parameter) and its robustness (thanks to Tyler's M-estimators).

B. Real data

In the case of the real data segmentation, we have extracted a fragment that has been slightly smoothed. This PolSAR image is shown in Figure 3, where at least three clusters can be distinguished. We again compare our results to the k-means and GMM clustering results. Segmented images are shown in Figure 4. In this case there is not a clear ground-truth and the results look similar. Results provided by GMM and R-EM are better than the ones obtained with the k-means. Then, it is difficult to compare GMM and R-EM since according to the region we consider conclusions are different, e.g. for the green cluster R-EM contains less misclassified pixels than GMM while conclusions are opposite for the purple cluster.

image	k-means	EM	R-EM
6-looked	0.85	0.92	0.92
9-looked	0.82	0.88	0.91
12-looked	0.96	0.98	0.99

Table I: Clustering accuracy of the different results

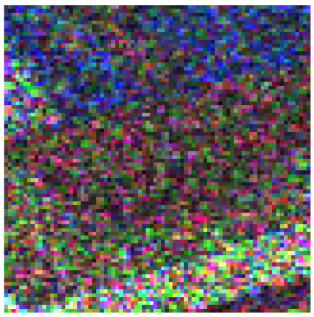

Figure 3: Real PolSAR image extract.

V. Conclusions

In this work, we have designed an original image segmentation method based on robust estimators that mimic the EM algorithm. We have performed experiments with MRF-based simulations of PolSAR images that have shown that our algorithm outperforms classical clustering techniques, namely the k-means and the EM algorithm for GMM distributions. On the other side, on real PolSAR data, results were more mitigated. In conclusion, this first work is promising and deserves to be analyzed more in depth since several parameters have to be tuned. Another interesting perspective would be to explore the complex case, more realistic for PolSAR images, directly by deriving new estimators from the complex likelihood. Finally, it would be interesting to derive an algorithm without assuming deterministic τ.

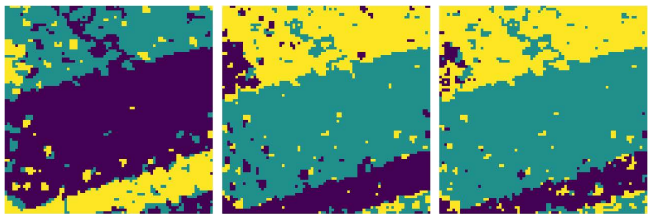

Figure 4: Segmentation results for k-means, GMM and R-EM applied to a 80×80 fragment of the real PolSAR image.

REFERENCES

[1] A. P. Dempster, N. M. Laird, and D. B. Rubin, "Maximum likelihood from incomplete data via the EM algorithm," *Journal of the Royal Statistical Society: Series B*, vol. 39, pp. 1–38, 1977.

[2] E. Conte and M. Longo, "Characterisation of radar clutter as a spherically invariant random process," *IEE Proceedings F - Communications, Radar and Signal Processing*, vol. 134, no. 2, pp. 191–197, 1987.

[3] F. Gini, M. V. Greco, M. Diani, and L. Verrazzani, "Performance analysis of two adaptive radar detectors against non-gaussian real sea clutter data," *IEEE Transactions on Aerospace and Electronic Systems*, vol. 36, no. 4, pp. 1429–1439, 2000.

[4] Huiguo Yi, Jie Yang, Pingxiang Li, Lei Shi, and Fengkai Lang, "A polsar image segmentation algorithm based on scattering characteristics and the revised wishart distance," *Sensors*, vol. 18, pp. 2262, 07 2018.

[5] Ying-Hua WANG and Chong-Zhao HAN, "Polsar image segmentation by mean shift clustering in the tensor space," *Acta Automatica Sinica*, vol. 36, no. 6, pp. 798 – 806, 2010.

[6] V. Roizman, M. Jonckheere, and Pascal Frédéric, "A flexible EM-like clustering algorithm for noisy data," *arXiv e-prints*, p. arXiv:1907.01660, Jul 2019.

[7] E. Ollila, D.E. Tyler, V. Koivunen, and H.V. Poor, "Complex elliptically symmetric distributions: Survey, new results and applications," *Signal Processing, IEEE Transactions on*, vol. 60, no. 11, pp. 5597–5625, November 2012.

[8] K Yao, "A representation theorem and its applications to spherically invariant random processes," *IEEE Trans.-IT*, vol. 19, no. 5, pp. 600–608, September 1973.

[9] D. E. Tyler, "A distribution-free M-estimator of multivariate scatter," *The Annals of Statistics*, vol. 15, no. 1, pp. 234–251, 1987.

[10] J. Frontera-Pons, M. Veganzones, F. Pascal, and J-P. Ovarlez, "Hyperspectral Anomaly Detectors using Robust Estimators," *IEEE Journal of Selected Topics in Applied Earth Observations and Remote Sensing (JSTARS)*, vol. 9, no. 2, pp. 720–731, february 2016.

[11] S. Foucher and C. López-Martínez, "Analysis, Evaluation, and Comparison of Polarimetric SAR Speckle Filtering Techniques," *IEEE Transactions on Image Processing*, vol. 23, no. 4, pp. 1751–1764, 2014.